Inverse kinematics proton scattering from the exotic nucleus ^{22}O

E. Becheva, E. Khan, Y. Blumenfeld, D. Beaumel, J.M. Daugas, F. Delaunay, C.E. Demonchy, A. Drouart, Muriel Fallot, A. Gillibert, et al.

Inverse kinematics proton scattering from the exotic nucleus ^{22}O

E. Becheva [a], E. Khan [a], Y. Blumenfeld [a], D. Beaumel [a], J.M. Daugas [b], F. Delaunay [a], Ch.-E. Demonchy [c], A. Drouart [d], M. Fallot[a], A. Gillibert [d], L. Giot [c], K.W. Kemper [e], D.T. Khoa [g], V. Lapoux [d], V. Lima [a], A. Musumarra [f], L. Nalpas [d], E. C. Pollacco [d], O. Roig [b], P. Roussel-Chomaz [c], J.-E. Sauvestre [b], J.A. Scarpaci [a], F. Skaza [d], H.S. Than [g]

[a] Institut de Physique Nucléaire, IN2P3-CNRS/Université Paris Sud, 91406 Orsay, France
[b] CEA Bruyères-le-Châtel Cedex 12, France
[c] GANIL, Bld Henri Becquerel, BP 5027, 14076 Caen Cedex, France
[d] SPhN, DAPNIA, CEA Saclay, 91191 Gif sur Yvette Cedex,France
[e] Departement of Physics, Florida State University, Tallahassee, Florida 32306
[f] INFN-Laboratorio Nazionale del Sud, Via S. Sofia 44, Catania, Italy
[g] INST, VAEC, P.O. Box 5T-160, Nghia Do, Hanoi, Vietnam

Abstract

We have measured for the first time elastic and inelastic proton scattering from the neutron rich nucleus ^{22}O at 46.6 AMeV using the MUST array. Angular distributions for elastic and inelastic scattering towards the 2_1^+ state have been extracted. Both a phenomenological and a microscopic analysis have been performed. The 2_1^+ state in ^{22}O is shown to exhibit an isovector character. The comparison with the data for other neutron-rich oxygen isotopes indicates a strong subshell closure at N=14.

1 Introduction

The investigation of long isotopic chains ranging from the neutron to the proton drip lines gives us a global view of the nuclear structure evolution. Such studies can constrain theoretical models of the nucleus, particulary concerning the potential and nucleon-nucleon effective force. In particular, the study of light neutron rich-nuclei during the last few years has highlighled new phenomena such as the appearance or disappearance of shell and subshell closures. The N=8 magic number is observed to disappear for Be [1, 2] and evidence for the disappearance of the N=20 shell is the non-existence of ^{26}O and ^{28}O [3, 4].
The oxygen isotopic chain plays a particular role among light nuclei. It contains one of the rare stable doubly magic nuclei, ^{16}O. Moreover, the last bound oxygen isotope was found to be ^{24}O [5, 6] while the last bound fluorine isotope was found to be ^{31}F. This suggests rapid structural changes for the oxygen isotopes as a function of a neutron number. Recent studies of ^{22}O nuclei [7, 8] have provided unexpected results. They measured the energy of the first 2_1^+ excited state to be E(2^+)=3.17 MeV [7, 8] and the quadrupole transition probability B(E2↑)=21±8 e^2fm^4 [7]. The systematics of the 2^+ state energy (Fig.1) for the oxygen isotopes shows that the energy decreases starting from ^{16}O to ^{20}O and increases for ^{22}O which suggests a subshell closure at N=14. This subshell closure is also supported by the B($E2\uparrow$) value (Fig.2) which is lower for ^{22}O than for ^{20}O. It should be noted, that this increase of E(2^+) energy wasn't observed for the neighboring isotopic chains of Carbon, Neon and Silicon. Reference [8] also observed an additional γ-ray at 1370 keV attributed to the decay of a state at 4.65 MeV towards the 2^+ state.
We report in this paper the experimental results of the ^{22}O(p,p') reaction at 46.6 AMeV. Phenomenological and microscopic analyses were undertaken.

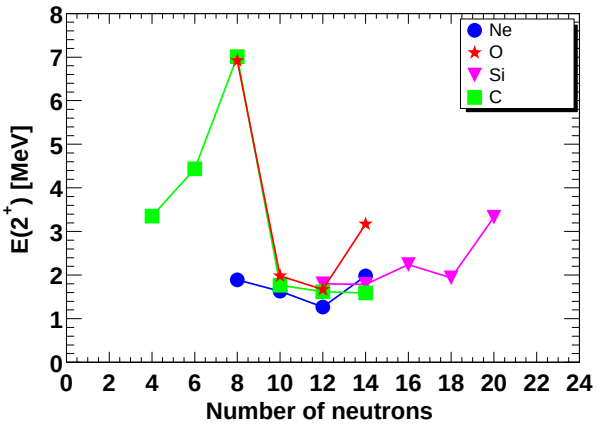

Figure 1: Systematics of 2_1^+ state energy for the isotopic chains with Z=6, Z=8, Z=10 and Z=14 as a function of a neutron number

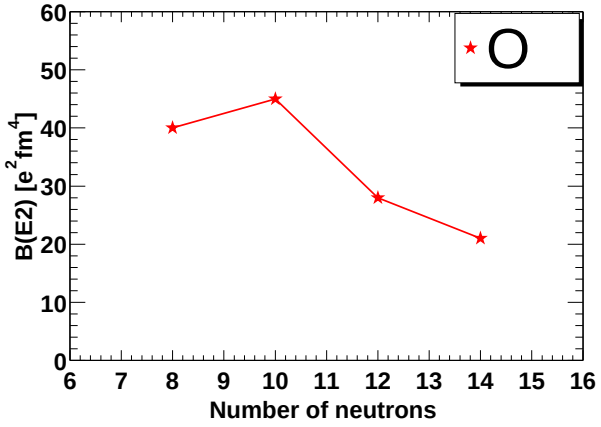

Figure 2: Systematics of B(E2↑) of the first 2^+ state for the oxygen isotopic chain as a function of a neutron number

2 Experimental method

2.1 Specificity of (p,p') reaction

The (p,p') reaction has been used since 50 years to study stable nuclei. In recent years, the development of experimental techniques involving radioactive beams has made possible the measurement of the (p,p') reaction in inverse kinematics with exotic nuclei. Proton elastic scattering yields information about the ground state matter densities. The inelastic scattering is used as a tool to obtain information on low-lying excited states. At energies of a few tens of MeV, inelastic proton scattering is mostly sensitive to the neutrons in the nucleus, and is therefore a very suitable tool to determine the ratio of transition matrix elements M_n/M_p by a comparaison with the deformation parameter obtained from electromagnetic excitation, which is only sensitive to the protons [9].

2.2 Experimental technique

The experiment was performed at the GANIL facility, Caen, France. A $^{36}S^{16+}$ primary beam with intensity of 3.10^{12} pps, was fragmented on a 440 mg/cm^2 ^{12}C target located in the SISSI device. We have obtained a cocktail beam containing around 1000 ^{22}O nuclei per second at 46.6 AMeV. The secondary beam impinged on a proton rich target $(CH_2)_n$ of $5mg/cm^2$ placed in the SPEG reaction chamber. The recoiling protons were detected in 8 telescopes of the MUST array [10] which measure the energy and angle of the recoiling protons. The telescopes were mounted on two columns (four detectors on each column) covering between 60 - 70 deg. and 65 - 75 deg. in the laboratory frame and placed at 15 cm from the target. This placing of the detectors ensured a maximum geometrical efficiency in the angular range of interest (15 to 45 deg. in the center-of-mass frame).
The nuclei scattered from the secondary beam were detected in the SPEG spectrometer. Due to the large emittence we had to track the secondary beam event by event. The aim is to reconstruct the exact interaction position on the target and thus, the right scattering angle of the protons. This feature plays an important role for the ^{22}O excitation energy resolution. For this purpose we used two MWPCs (CATS) [11] developed by CEA Saclay. These detectors are placed upstream from the reaction target at 1.6 m and 0.5 m and give us a two dimensional location of the passage point of a nucleus through the detector plane. The resulting position resolution on the target is about 1mm.
The recoiling protons were detected in the MUST detector array. One MUST telescope consists of three stages : a double sided Si-strip detector, a Si(Li) detector and CsI(Tl) cristal. The protons with an energy less than 6 MeV were identified by TOF - Energy in the double sided Si strip detector. The protons with an energy greater than 6 MeV were identified by $\Delta E - E$ technique using the energy loss in the three stages. Fig.3 displays a typical $\Delta E - E$ identification matrix using the energy loss in a double sided Si strip and a Si(Li) detector.
The ^{22}O nuclei are identified by their energy loss in the SPEG gas ionization chamber and TOF between one MWPC (CATS) and a plastic scintillator placed at the exit of the SPEG spectrometer.

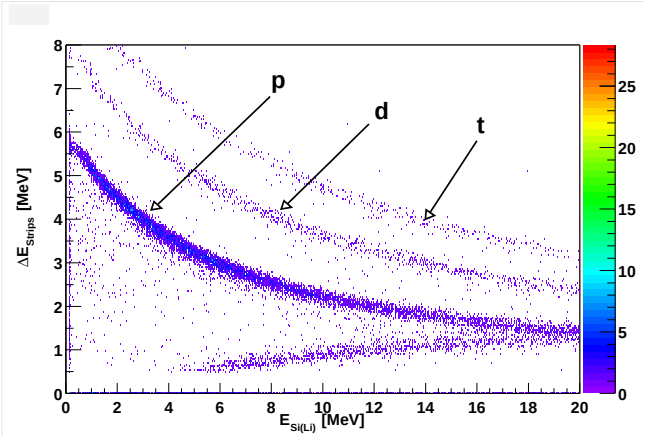

Figure 3: Typical ΔE-E identification matrix for the protons.

Fig.4 displays an identification plot of scattered secondary beam nuclei. The secondary beam contains also neutron-rich nuclei ^{23}F and ^{25}Ne. We extract

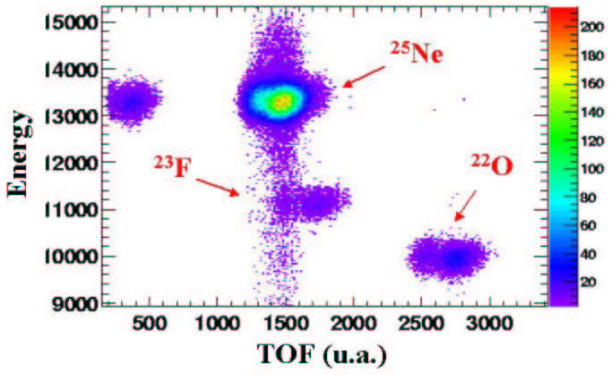

Figure 4: Identification matrix for the secondary beam nuclei using the energy loss in a gas ionization chamber and TOF technique.

the events in which a proton is detected in coincidence with an ^{22}O nucleus.

3 Experimental results

Information about the ^{22}O(p,p') reaction is obtained directly by using the measured proton energy and recoiling angle θ_p. For the calculation of θ_p we reconstruct a beam trajectory using two MWPC detectors and take into account the interaction position on the target. The proton energy is corrected for the energy loss in the target. Fig.5 displays a scatterplot showing the proton energy versus scattering angle in the laboratory frame. The very intense line corresponds to the ground state of ^{22}O. The second line located at smaller angles shows events corresponding to the first excited state of ^{22}O. The broadening at low proton energy is due to the straggling in the target. The excitation en-

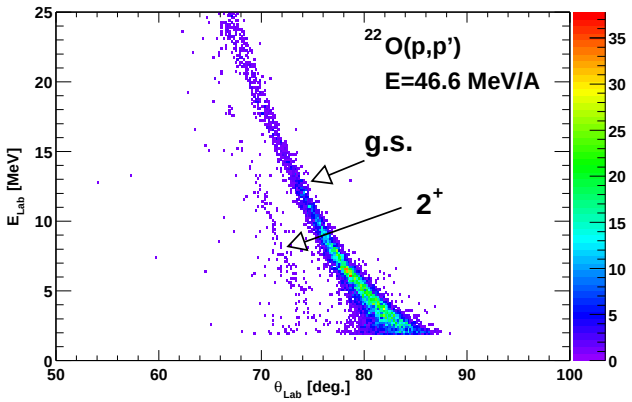

Figure 5: Recoiling proton energy versus angle scatterplot in the laboratory frame for the ^{22}O(p,p') reaction for 46.6 MeV/A beam energy

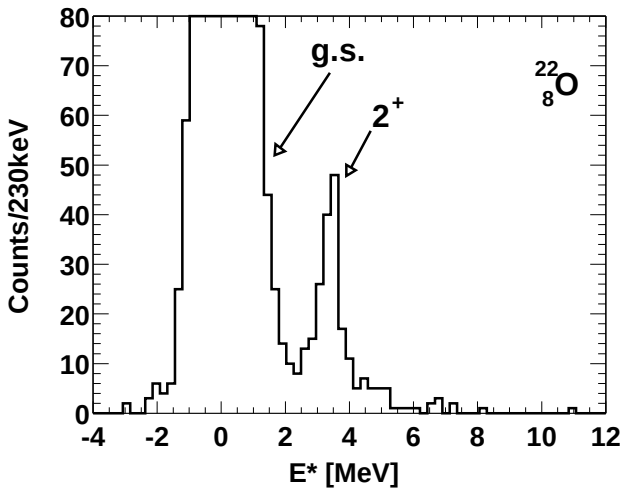

Figure 6: Excitation energy spectra for ^{22}O

ergy and center-of-mass scattering angle were deduced using two-body relativistic kinematics. Fig.6 shows the excitation energy spectrum of ^{22}O. The ground state and 2_1^+ peaks are clearly visible. The resolution of the elastic peak is approximately 800 keV which depends mainly on the angular resolution of the scattering angle measurements for the protons, the angular straggling in the target and the resolution of the position measurement. The 2_1^+ state is located at 3.24 ± 0.20 MeV, which is in very good agreement with the value found by [7]. We extracted the angular distribution of the cross section (Fig.7) for the g.s. and the 2_1^+ state making

the cuts around the corresponding peaks (-2 MeV and 2.4 MeV for the g.s. and 2.4 MeV - 4.2 MeV for the 2_1^+ state).

4 The phenomenological analysis

To analyse the experimental angular distributions we have used as a first approach a phenomenological analysis. We performed a CCBA calculation using ECIS88 code [12]. Here we use the Becchetti and Greenlees [13] parameterization for the proton-nucleus interaction optical potential. This parameterization depends only on A, Z and on the nucleus energy. The results are displayed in a solid lines in Fig.7. For the ground state angular distribution we have an overall reproduction the data but a sizeable disagreement is clearly seen at large angle. A deformation parameter $\beta_{pp'}$=0.26±0.04 was extracted by normalizing the calculated inelastic angular distribution to the data. The errors bar correspond to the minimum and maximum $\beta_{pp'}$ values which allow the measured angular distribution to be reproduced within 1-sigma. In spite of the fact that we have a good agreement for the 2_1^+ state data confidence in this optical potential is questioned for ^{22}O.

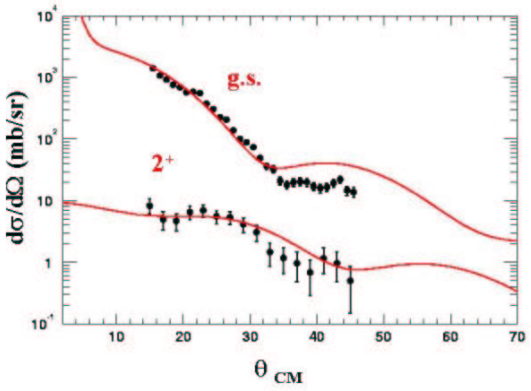

Figure 7: 46.6 MeV/A (p,p') ^{22}O elastic and inelastic angular distribution for the ground and 2_1^+ states. The experimental data are shown in dottes and solid lines corresponds to a DWBA calculation using a Becchetti-Greenlees optical potential. The error bars are purely statistical.

It should be noted, that the Becchetti-Greenlees parameterization was derived using angular distribution systematics for stable nuclei. It was also used with success for some neutron rich nuclei such ^{18}O and ^{20}O [14], ^{30}S, ^{34}Ar [15], or $^{38,40}S$, ^{43}Ar [16, 17]. For ^{22}O we see a first failure of this parameterization when approaching the drip line. Thus it becomes necessary to calculate the optical potential from the more fundamental quantities such as the neutron and proton densities and a nucleon-nucleon interaction.

5 The microscopic analysis

The elastic and inelastic data were analyzed in the Distorted Wave Born Approximation (DWBA) using nucleon-nucleus elastic and transition potentials obtained by folding [18] the nuclear ground state [19] and transition densities [20] with the DDM3Y interaction. The imaginary optical potential was parametrized in Woods-Saxon form using the recent phenomenological optical model potentials [21]. Fig.8 displays microscopic calculations for the ground and 2^+ state angular distributions. The elastic data are very well reproduced while the inelastic data are overestimated by the QRPA transition density. In should be noted that ^{18,20}O+p scattering data have been analyzed with success by the optical model using a real folded potential [22].

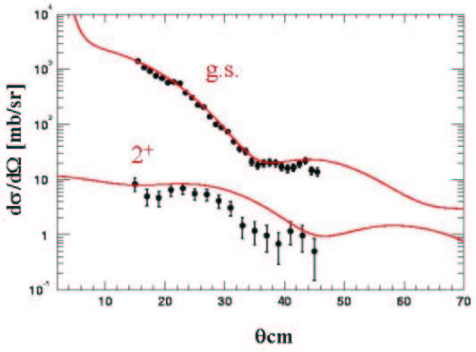

Figure 8: Elastic and inelastic $^{22}O + p$ scattering data at 46.6 MeV/nucleon compared with the DWBA cross sections obtained with microscipic optical and transition potentials (see text)

Neutrons and protons may contribute in different ways to the 2_1^+ excitation [9]. This can be expressed by the M_n/M_p ratio where $M_{n(p)}$ is a transition matrix element for the neutrons

(protons). The experimental M_p value is given by the measurement of B(E2↑) [7] using the relation $|M_p|^2 = \mathrm{B(E2\uparrow)/e^2}$. We have calculated M_p using the proton transition density calculated by the continuum QRPA approach and the relation

$$M_p = \int_0^{+\infty} \rho^p_{\lambda fi}(r) r^{\lambda+2} dr$$

where $\rho^p_\lambda(r)$ is a proton transition density for the quadrupole excitation ($\lambda = 2$). The microscopic value of M_p found in this manner, ($|M_p|$=4.69 fm^2) is in very good agreement with the experimental data. The M_n value is then deduced by renormalizing the neutron transition density in order to reproduce the experimental data for the inelastic angular distribution. In this way, we have obtained the very preliminary value $\mathrm{M}_n/\mathrm{M}_p = 2.5 \pm 0.5$.

6 Discussion

In a usual collective model, the protons and neutrons form a homogeneous fluid where the protons and neutrons move in phase. In such a picture, the proton and neutron multipole matrix elements obey to the relationship M_n/M_p=N/Z. Bernstein et al. [23] performed a systematic examination of M_n/M_p values for $0^+_{gs} \rightarrow 2^+_1$ transitions in even-even single-closed-shell nuclei and found that the closed proton shell nuclei generally have a $M_n/M_p > N/Z$, while closed neutron shell nuclei have $M_n/M_p < N/Z$. Strong deviations of the M_n/M_p value from N/Z could indicate a shell or subshell closure. The M_n/M_p values for the neutron rich oxygen isotopes $^{18-22}$O are given in table 1.

	β_C	$(M_n/M_p)_{2^+}$	N/Z
^{18}O	0.355(8) [24]	1.10(24) [14]	1.25
^{20}O	0.261(9) [24]	3.25(0.80) [14]	1.5
^{22}O	0.21(4) [7]	2.5	1.75

Table 1: Coulomb deformation parameter β_C and M_n/M_p values for 2^+_1 state of $^{18-22}O$

These systematics show that the M_n/M_p value increases from ^{18}O to ^{20}O and decreases from ^{20}O to ^{22}O. It should be noted that the proton density deformation seems to decrease when N increases: the presence of more and more neutrons inhibits the proton deformation. The low M_n/M_p value of ^{18}O could be explained by a high M_p value as suggested by the β_C value. This strong proton excitation could be interpreted as a core polarisation effect. Considering the ^{18}O nucleus as ^{16}O+2n, the ^{16}O core is polarized by the presence of 2n. On the other hand, the core polarization effect is reduced in ^{22}O as confirmed by the β_C value. This could be due to the N=14 subshell closure. Finally, for ^{20}O the high M_n/M_p value is mostly due to a strong neutron contribution, since the β_C value is not especially small. This difference of behavior compared to ^{18}O, is still an open question. Moreover the QRPA calculations [14] for B(E3) suggest a strengthening of the proton shell closure for Z=8, especially for ^{24}O. This would imply an even smaller core polarisation effect for ^{24}O.

7 Conclusion

In summary, we have measured angular distributions for elastic and inelastic scattering of protons in inverse kinematics from the neutron rich nucleus ^{22}O. We found the energy of the first excited state 2^+_1 to be 3.24 ± 0.20MeV which is in good agreement with a value measured in previous experiments [7, 8]. Good quality angular distribution were obtained for elastic and inelastic scattering with a low beam intensity of 1000 pps. We observed a failure of phenomenological analysis using the Becchetti and Greenlees parameterization to reproduce the large angle elastic data. The microscopic approach gives a preliminary value of M_n/M_p=2.5 for the 2^+_1 excitation. The comparison with the data for the ^{18}O and ^{20}O nuclei reflects a subshell closure for N=14 but the structural evolution is not yet fully understood. It is clear that additional work looking for the first excited state of ^{24}O must be done to get a greater understanding of the nuclear structure evolution in this region of the nuclear chart.

References

[1] A. Navin et al., Phys. Rev. Lett. 85 (2000) 266

[2] H. Iwasaki et al., Eur. Phys. J. A13 (2002) 55

[3] D. Guillemaud-Muller et al., Phys. Rev.C41 (1990) 937

[4] M. Fauerbach et al., Phys. Rev. C53 (1996) 647

[5] O. Tarasov et al., Phys. Lett. B 409 (1997) 64

[6] H. Sakurai et al., Phys. Lett. B 448 (1999) 180

[7] P.G. Thirolf et al., Phys. Lett. B 485 (2000) 16

[8] M. Belleguic et al., Nucl. Phys. A 682 (2001) 136c

[9] A.M. Bernstein et al., Comments Nucl. Part. Phys. 11 (1983) 203

[10] Y. Blumenfeld et al., Nucl. Instr. Meth. Phys. Res. A 421 (1999) 471

[11] S. Ottini-Hustache et al.,Nucl. Instr. Meth. Phys. Res. A 431 (1999) 476

[12] J. Raynal, Phys. Rev. C 23 (1981) 2571

[13] F.D. Becchetti, G.W. Greenlees, Phys. Rev. 182 (1969) 1190

[14] E. Khan et al., Phys. Lett. B 490 (2000) 45

[15] E. Khan et al., Nucl. Phys. A 694 (2001) 103

[16] J.H. Kelley et al., Phys. Rev. C 56 (1997) 1206

[17] F. Marechal et al., Phys. Rev. C 60 (1999) 064623

[18] Dao T. Khoa et al., Nucl. Phys. A 706 (2002) 61

[19] M. Grasso et al., Phys. Rev. C 64 (2001) 064321

[20] E. Khan et al., Phys. Rev. C 66 (2002) 024309

[21] A.J. Koning and J.P. Delaroche, Nucl. Phys. A 713 (2003) 231

[22] Dao T. Khoa, Phys. Rev. C 68, (2003) 011601(R)

[23] A. M. Bernstein et al., Phys. Lett. 103B (1981) 255

[24] S. Raman et al., ADNDT 36 (1987)